micro

MDPI

*Article*

# Sinapic Acid Release at the Cell Level by Incorporation into Nanoparticles: Experimental Evidence Using Biomembrane Models

**Cristina Torrisi, Arianna Morgante, Giuseppe Malfa, Rosaria Acquaviva, Francesco Castelli, Rosario Pignatello and Maria Grazia Sarpietro ***

Department of Drug and Health Sciences, University of Catania, Viale Andrea Doria 6, 95125 Catania, Italy; torrisi.cristina@hotmail.it (C.T.); ariannamorgante@hotmail.it (A.M.); g.malfa@unict.it (G.M.); racquavi@unict.it (R.A.); fcastelli@unict.it (F.C.); r.pignatello@unict.it (R.P.)

* Correspondence: mg.sarpietro@unict.it; Tel.: +39-0957384260

**Abstract:** Sinapic acid (SA), belonging to the phenylpropanoid family, and its derivatives are secondary metabolites found in the plant kingdom. In recent years, they have drawn attention because of their various biological activities, including neuroprotective effects. In this study, SA was incorporated into two different nanoparticle systems, solid lipid nanoparticles (SLN) and nanostructured lipid carriers (NLC). The influence of different concentrations of SA on the nanoparticle systems was evaluated. It was studied the efficacy of the nanoparticle systems to release the active ingredient at cell level through the use of models of biological membranes represented by multilamellar vesicles (MLV) of dimyristoylphosphatidylcholine (DMPC) and conducting kinetic studies by placing in contact SLN and NLC, both unloaded and loaded with two different amounts of SA, with the same biological membrane model. Differential scanning calorimetry (DSC) was used for these studies. The results indicated a different distribution of SA within the two nanoparticle systems and that NLC are able to incorporate and release SA inside the structure of the biological membrane model.

**Keywords:** lipid nanocarriers; SLN; NLC; DSC; liposomes; MLV



**Citation:** Torrisi, C.; Morgante, A.; Malfa, G.; Acquaviva, R.; Castelli, F.; Pignatello, R.; Sarpietro, M.G. Sinapic Acid Release at the Cell Level by Incorporation into Nanoparticles: Experimental Evidence Using Biomembrane Models. *Micro* **2021**, *1*, 120–128. https://doi.org/10.3390/micro1010009

Academic Editor: Horacio Bach

Received: 29 June 2021
Accepted: 27 July 2021
Published: 31 July 2021



## 1. Introduction

Various secondary plant metabolites were evidenced to have beneficial activity on several pathological conditions [1–4]. Among these positive effects, many studies have revealed different neuroprotective mechanisms for natural compounds [5], which doubtless represent a more than a valid tool in the prevention strategy.

Phytochemicals play in fact a key role in maintaining the brain homeostasis by influencing receptor functions and counteracting oxidative stress [6,7]. Recently, Sinapic acid (SA) and its derivatives have drawn attention because of their various biological activities including anti-inflammatory, anti-cancer and neuroprotective effects, with promising potential for the treatment of neurodegenerative and neuropsychiatric disorders [8–11]. SA is one of the most common compounds of the class of hydroxycinnamic acids, together with caffeic acid and ferulic acid. It is widespread in the plant kingdom and is mainly found in citrus, berry fruits, cereals and vegetables, and is one of the characteristic compounds of the *Brassicaceae* family [12]. SA, as well as all hydroxycinnamic acid derivatives, is able to neutralize the free radical species through the formation of more stable phenoxyl radicals, resulting in a potent antioxidant effect comparable to that of caffeic acid, and higher than ferulic acid and hydroxycinnamic acid [9].

Plant biosynthesis starts from the amino acids phenylalanine and tyrosine as precursor molecules and proceeds to the shikimate pathway that, after different enzymatic processes, produces hydroxycinnamic acid derivatives, including SA [12]. It can be found in free form or conjugated with sugar (glycosides) or as esters with organic compounds [13].

Different factors affect the bioavailability of natural compounds and the accessibility of these various molecules through the target tissues and reduces the already low and still not well-defined bioavailability, especially across the blood–brain barrier (BBB) [14]. Therefore, in order to optimize polyphenols in terms of efficiency, specificity and safety, the controlled target delivery to central nervous system (CNS) or to other target area is an urgent need. In this research, we studied two different lipid-based nanocarrier systems, namely solid lipid nanoparticles (SLN) and nanostructured lipid carriers (NLC), to verify their ability to load and release SA at a cell level. Multi-lamellar vesicles (MLV) made of dimyristoylphosphatidylcholine (DMPC) was adopted as a well-validated system for mimicking the biological membrane characteristics [15,16]. The influence of drug concentration on the morphology of the lipid systems, and kinetic studies in the presence of unloaded and loaded SLN and NLC were conducted together with the evaluation of the potential release of SA by following changes in the thermotropism of the resulting lipid/liposomal systems.

## 2. Materials and Methods

### *2.1. Materials*

Cethyl palmitate (Cutina, CP), glyceril oleate (Tegin O), Oleth-20 and isopropyl myristate were obtained from A.C.E.F. S.p.a (Piacenza, Italy). Sinapic acid was provided by Sigma-Aldrich (Milan, Italy). Dimyristoylphospatidylcholine (DMPC) was obtained from Genzyme (Liestal, Switzerland).

### *2.2. SLN and NLC Preparation*

SLN and NLC were prepared by the phase inversion temperature method. Their composition is reported in Table 1. The lipid phase (Cutina, Oleth-20, Tegin O) was melted at about 85 °C. SA was added to the lipid phase. The aqueous phase was warmed at 85 °C and added dropwise to the lipid phase, under agitation. At the phase inversion temperature, the preparation was transparent and a O/W system was obtained. The sample was left under agitation up to room temperature [17]. Isopropyl myristate was added to the lipid phase for NLC preparation. Blank SLN and NLC without SA were also prepared.

**Table 1.** Composition of SLN and NLC.

| Sample | Cutina (g) | Tegin O (g) | Oleth-20 (g) | Isopropyl Myristate (g) | SA (g) | $H_2O$ (g) |
|---|---|---|---|---|---|---|
| SLN | 1.400 | 0.880 | 1.720 | - | - | qb 20 |
| SLN SA 1% | 1.400 | 0.880 | 1.720 | - | 0.014 | qb 20 |
| SLN SA 5% | 1.400 | 0.880 | 1.720 | - | 0.070 | qb 20 |
| NLC | 1.220 | 0.772 | 1.520 | 0.500 | - | qb 20 |
| NLC SA 1% | 1.220 | 0.772 | 1.520 | 0.500 | 0.012 | qb 20 |
| NLC SA 5% | 1.220 | 0.772 | 1.520 | 0.500 | 0.061 | qb 20 |

- the component is not present.

### *2.3. Particle Size Determination*

SLN and NLC particle size and polydispersity index (PdI) was determined at room temperature using a Zetasizer Nano ZS 90 (Malvern Instruments, Malvern, UK), by light scattering at 90°. The instrument performed particle sizing by means of a 4 mW laser diode operating at 670 nm. The values of the mean diameter and polydispersity index were the averages of results obtained for three replicates of two separate preparations.

### *2.4. Stability Tests*

The SLN and NLC samples were stored in airtight jars and then kept in the dark at room temperature and at 37 °C for two months, separately. Particle size and PdI of each sample were measured and calorimetric analyses were also carried out (as described in

Section 2.8.1. Nanoparticles and MLV analysis) at fixed time intervals (24 h, one week, two weeks, three weeks, one month, and two months) after their preparation.

### *2.5. Nanoparticle Freeze-Drying*

SLN and NLC suspensions were kept for at least 24 h at −20 °C and then submitted to the lyophilization process for 48 h in a Labconco, FreeZone freeze drier (Kansas City, MO, USA).

### *2.6. Preparation of MLV*

DMPC was solubilized (40 mg/mL) in chloroform/methanol (1:1; *v*/*v*). Aliquots of the solution containing 7 mg of DMPC were delivered in glass tubes. The solvents were evaporated off under a nitrogen flux; any solvent residue was eliminated by freeze-drying. Then, 168 µL of 50 mM Tris buffer (pH = 7.4) was added to the phospholipid films. The samples were kept at 37 °C for 1 min and vortexed for 1 min, for three times. Finally, the samples were kept at 37 °C for 60 min.

### *2.7. Preparation of MLV Containing SA*

DMPC and SA were separately solubilized in chloroform/methanol (1:1, *v*/*v*). Aliquots of the DMPC solution (7 mg of DMPC) were poured in glass tubes. Aliquots of the SA solution were added to the glass tubes in order to have the same amount of SA in the nanoparticles used for the interaction between nanoparticles and MLV. Then, the samples were treated as described in Section 2.6. The vesicle samples contained 0.15 mg SA/mL and 0.76 mg SA/mL, respectively.

### *2.8. DSC Analysis*

Calorimetric analysis was carried out using a DSC1 Mettler Toledo STARe (Greifensee, Switzerland). Data acquisition was obtained by the Mettler TA-STAR software (version 16.00). Calorimetric aluminum pans of size 160 µL calorimetric aluminum pans were used. The reference pan contained 120 µL of distilled water. The instrument was calibrated using indium (99.95% purity).

#### 2.8.1. Nanoparticles and MLV Analysis

Samples (120 µL) were put into the calorimetric aluminum pan, hermetically closed and submitted to the following analysis: heating from 5 °C to 70 °C, 2 °C/min; cooling from 70 °C to 5 °C, 4 °C/min three times.

#### 2.8.2. Analysis of the Interaction between SLN/NLC and MLV

A total of 30 µL SA-loaded SLN or NLC and 90 µL of MLV were put into a calorimetric pan that was sealed and submitted to DSC analysis as follows: (1) heating scan from 5 °C to 70 °C (2 °C/min); (2) cooling scan from 70 °C to 37 °C (4 °C/min); (3) isothermal scan at 37 °C, 60 min; (4) cooling scan from 37 °C to 5 °C (4 °C/min). The procedure was repeated eight times in order to evaluate the interaction between nanoparticles and MLV during time [18]. Experiments with unloaded nanoparticles were also carried out.

## 3. Results and Discussion

### *3.1. Particle Size Determination and Stability Evaluation*

All the tested formulations showed a mean particle diameter in the range of 30–51 nm, and a single peak in size distribution (Table 2). Particle size, PdI and calorimetric analysis have highlighted that nanoparticle characteristics remain unchanged over the time indicated.

**Table 2.** Average size and polydispersity index (PdI) of SLN and NLC with and without SA.

| Sample | Size ± S.D. (nm) | PdI ± S.D. |
|---|---|---|
| SLN | 29.6 ± 0.6 | 0.296 ± 0.06 |
| SLN SA 1% | 36.3 ± 1.1 | 0.303 ± 0.062 |
| SLN SA 5% | 35.6 ± 0.6 | 0.380 ± 0.046 |
| NLC | 27.6 ± 8.0 | 0.352 ± 0.034 |
| NLC SA 1% | 31.9 ± 7.8 | 0.398 ± 0.054 |
| NLC SA 5% | 35.7 ± 2.2 | 0.272 ± 0.043 |

### *3.2. DSC Analysis of Nanoparticles*

SLN and NLC have been analyzed by DSC. Figure 1 shows the calorimetric curves of Cutina, SLN and NLC. Cutina shows a calorimetric peak at about 53.8 °C and a shoulder at about 42 °C. The SLN show a peak at about 46 °C. The NLC show a peak at approximately 44 °C. The endothermic peaks of SLN and NLC occur at a lower temperature than pure Cutina, suggesting that the latter was in a less ordered state within the nanoparticles. The temperature drip of the NLC peak compared to the SLN one was due to the insertion of the liquid lipid in the NLC, causing a lower order state in the nanoparticle structure. In both SLN and NLC systems, shoulders were visible at higher and lower temperatures, which could be due to an uneven distribution among the components of nanoparticles [17].

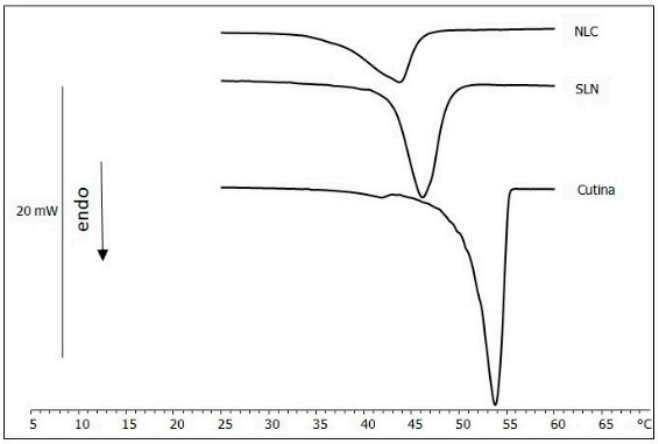


**Figure 1.** Calorimetric curves, in heating mode (temperature increase), of Cutina, SLN and NLC. The arrow (endo) indicates that the process is endothermic.

The calorimetric curves, in heating mode, of SLN prepared without and with 1% and 5% SA are shown in Figure 2A. Compared to the peak of unloaded SLN, the peak of SLN SA 1%, showed a slight enlargement, while the peak of SLN containing 5% SA showed a significant enlargement. This indicates that 1% SA only slightly affects the structure of SLN; instead, at a higher concentration, SA influences the order of the SLN structure, by inserting itself among the molecules of the lipids, causing a reduction in the molecular cooperativity during melting. The calorimetric curves of NLC without and with SA are shown in Figure 2B. SA highly influences the calorimetric curve of NLC. Already, at a 1% concentration, SA caused a widening of the peak and, at a lower temperature, the appearance of a shoulder. In the presence of 5% SA, the peak further widened and the shoulder evolved into a real endothermic peak to the detriment of the main peak, the intensity of which decreased. These results were a clear indication of the presence of the SA inside the NLC. SA determined a fluidification of the nanoparticle system, as indicated by the peak at lower temperatures, and a decrease in the cooperativity of the molecules during the transition phase from the ordered to the disordered state. The comparison of the calorimetric curves of SLN and NLC containing SA allows us to hypothesize a different disposition of the compound in the lipid matrix. In the SLN, SA could form domains between the solid lipid molecules; conversely, inside the NLC, SA could be distributed

more evenly between the molecules of the nanoparticle lipid phase. To ensure that the SA was completely localized inside the nanoparticles, the latter were freeze-dried and the obtained dry samples were also subjected to DSC analysis. The calorimetric curves of lyophilized NLC have been compared with the calorimetric curve of SA. SA shows an endothermic peak at 194.29 °C. In the NLC calorimetric curves, with 1% and 5% SA, there was no evidence of the SA peak (data not shown). This indicates that the SA lost its crystalline structure and was allocated inside the nanoparticles in an amorphous form [19].

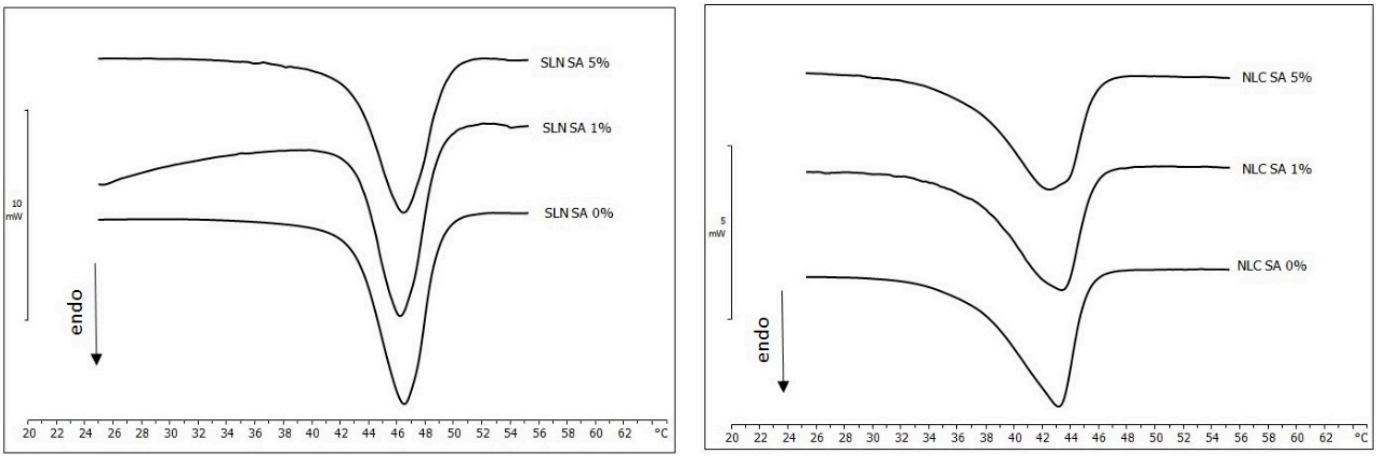


(**A**) (**B**)

**Figure 2.** Calorimetric curves, in heating mode (temperature increase), of (**A**) unloaded SLN and 1% and 5% SA-loaded SLN and (**B**) unloaded NLC and 1% and 5% SA-loaded NLC. The arrow (endo) indicates that the process is endothermic.

### *3.3. Analysis of the Interaction of SLN and NLC with MLV*

We wanted to study the interaction of SLN and NLC with biological membranes. To carry out the experiments we used MLV made of pure DMPC, a simplified system that effectively mimics many of the properties of biomembranes [16,20]. When MLV are heated, the double phospholipid layer undergoes a transition from the ordered (gel) phase to a ripple phase, and, therefore, from the ripple phase to a disordered (liquid–crystalline) phase. These transitions take place at a very precise temperature ($T_m$) and are characterized by a specific enthalpy change value ($\Delta H$). If a foreign compound interacts with the MLV, it causes variations of $T_m$ and/or $\Delta H$.

In this study, MLV were put into contact with lipid nanoparticles for about 12 h. The calorimetric curves, in heating mode, recorded at regular time intervals, are shown in Figures 3 and 4 and are compared with the calorimetric curves of empty MLV and of the pure nanoparticles. The calorimetric curve of MLV is characterized by a pretransition peak at about 17 °C (relative to the passage from the ordered phase to the ripple phase) and by a main transition peak at about 25 °C (relative to the transition from the ripple phase to the disordered phase) [21,22]. The calorimetric curves of the MLV put in contact with the unloaded SLN are shown in Figure 3A. The SLN signal remained almost unchanged over time, while the MLV signal underwent considerable variations: in fact, the pre-transition peak disappeared and the main transition peak gradually became smaller. This indicates that the SLN can interact with the MLV. With regard to the experiments performed with unloaded NLC (Figure 3B), it was clearly noted that the MLV peak underwent some variations: in fact, it shrank and became progressively smaller. Additionally, the pre-transition peak disappeared and the NLC peak slightly widened. These results indicate that the NLC are capable to interact with the MLV keeping their structure almost unchanged. In particular, NLC could be included between the double phospholipid layers of MLV, as indicated by the decrease in peak intensity of the MLV.

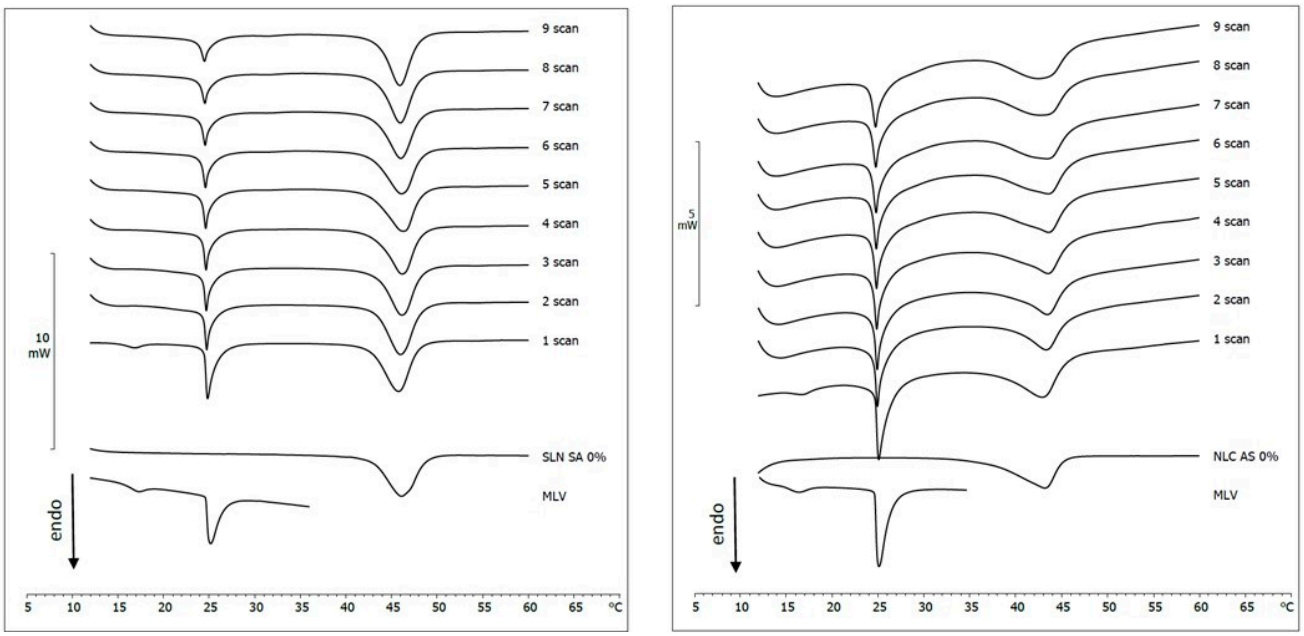


(**A**) (**B**)

**Figure 3.** Calorimetric curves, in heating mode (temperature increase), of MLV left in contact with (**A**) unloaded SLN; the calorimetric curves are compared with MLV and SLN calorimetric curves, and (**B**) unloaded NLC; the calorimetric curves are compared with the calorimetric curves of MLV and NLC. The arrow (endo) indicates that the process is endothermic.

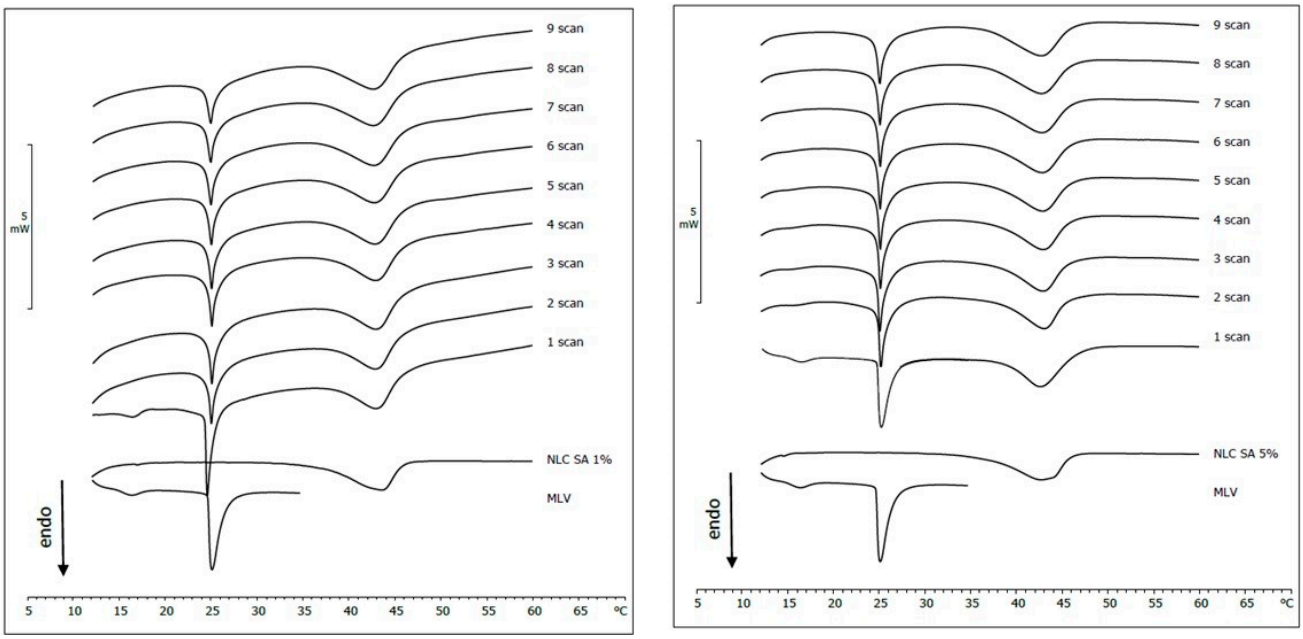


(**A**) (**B**)

**Figure 4.** Calorimetry curves, in heating mode (temperature increase), of MLV left in contact with (**A**) 1% SA-loaded NLC; the calorimetric curves are compared with the calorimetric curves of MLV and 1% SA-loaded NLC. (**B**) 5% SA-loaded NLC; the calorimetric curves are compared with the calorimetric curves of MLV and 5% SA-loaded NLC. The arrow (endo) indicates that the process is endothermic.

To check if even the NLC containing SA were able to interact with MLV and release SA within the MLV, we repeated the DSC experiments incubating the MLV with the drug-loaded lipid systems. The calorimetric curve, in heating mode, obtained (Figure 4A) using

NLC, containing 1% SA, show that the MLV peak became smaller and smaller and shrank; compared to the NLC DSC curve, the lower temperature shoulder disappeared from the first scan and a single peak was registered. The behavior of MLV and NLC containing 5% SA was analogous (Figure 4B). In fact, in this case, the peak relative to MLV also got smaller and thinner; instead, the signal related to the NLC lost the shoulder at a lower temperature, creating a single peak. The large peak variation of MLV indicates that even NLC containing SA are able to fit into the structure of MLV; the loss of the shoulder at a lower temperature of the NLC signal suggests that the NLC is able to release SA into the MLV.

To acquire more information, the variation in the transition enthalpy, expressed as $\Delta\Delta H/\Delta H^0$ ($\Delta\Delta H = \Delta H - \Delta H^0$, where $\Delta H$ is the enthalpy variation of DMPC MLV in the presence of each of the systems analyzed and $\Delta H^0$ is the enthalpy variation of pure DMPC MLV) has been reported as a function of the calorimetric scans (Figure 5). All systems caused a lowering of the enthalpy variation in the MLV peak. However, the level of the decrease varied as a function of the system analyzed in the following order: unloaded NLC < NLC SA 1% < NLC SA 5%. These results indicate that, in the experiments with NLC containing SA, the effect on enthalpy variation could be due to both NLC and SA released by NLC.

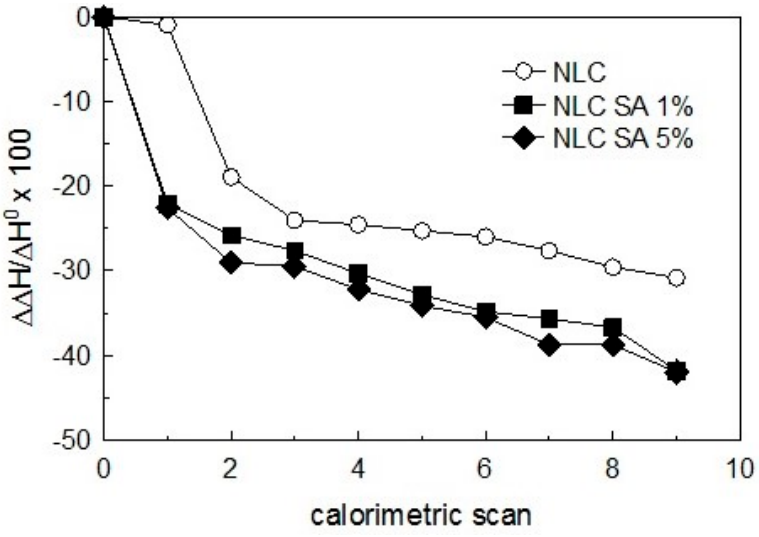


**Figure 5.** Transition enthalpy variation of MLV left in contact with unloaded NLC, with 1% SA-loaded NLC and with 5% SA-loaded NLC, as a function of the calorimetry scans. The transition enthalpy variation is reported as $\Delta\Delta H/\Delta H^0$ ($\Delta\Delta H = \Delta H - \Delta H^0$, where $\Delta H$ is the transition enthalpy variation in the MLV in the presence of each of the systems under analysis and $\Delta H^0$ is the transition enthalpy variation of pure DMPC MLV).

To confirm this hypothesis, the interaction of MLV with pure SA was investigated.

### *3.4. MLV/Sinapic Acid Interaction*

These experiments were carried out to try to explain the behavior of MLV brought into contact with NLC and with NLC loading SA. The MLV were prepared in the presence of SA so that the amounts of drug were the same as those present in the 1% and 5% NLC, respectively, which were put into contact with MLV in the MLV/NLC interaction experiments. The MLV obtained were subjected to calorimetric analysis and the obtained curves, in heating mode, are shown in Figure 6. SA did not cause large variations in the calorimetric curve of MLV: the pre-transition peak was present at both the concentrations of SA; the temperature of the main peak remained almost unchanged, while the enthalpy variation decreased. This indicates that the SA entering the MLV did not affect the fluidity of the system but has an effect on its stability. A compound can be located between the phospholipid chains as an "interstitial impurity" without causing changes of the

enthalpy and, therefore, without lowering the stability of the lipid membrane, or either as a 'substitute impurity' influencing the packaging of phospholipids and thus decreasing the stability of the double phospholipid layers [23,24]. SA, therefore, could behave as a substitute impurity causing changes in phospholipid packaging of MLV. These results confirm the hypothesis that NLC entered the structure of the MLV and released the carried SA inside them.

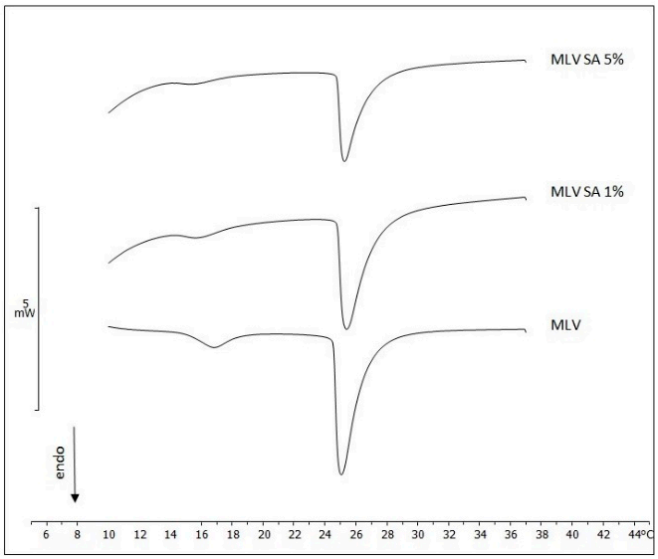


**Figure 6.** Calorimetric curves, in heating mode (temperature increase), of unloaded MLV and SA-loaded MLV. The amounts of SA in the MLV was equal to that present in the NLC loaded with SA and left in contact with MLV in the MLV/NLC interaction experiments. The arrow (endo) indicates that the process is endothermic.

## 4. Conclusions

SLN consisting of Cutina as solid lipid, oleth-20 (non-ionic surfactant) and glyceryl oleate (co-surfactant) have been prepared by using the PIT method. Isopropyl myristate, a liquid lipid, was further added to obtain the NLC. The nanoparticles were loaded with two different amounts of SA (1% and 5%). The presence of SA within the nanoparticle systems was demonstrated by calorimetric analysis on freeze-dried nanoparticles. The calorimetric analysis of nanoparticles samples indicated a better distribution of SA within the more disordered structure of NLC, compared to SLN. Calorimetric analysis allowed us to hypothesize that NLC are capable of being incorporated into the structure of the MLV (used as a biomembrane model) and to release SA into the MLV. These NLC could, therefore, be regarded as a promising carrier to improve the penetration of SA into cells.

**Author Contributions:** Conceptualization, M.G.S. and F.C.; methodology, M.G.S., R.A. and R.P.; software, C.T. and A.M.; validation, M.G.S., R.A. and F.C.; formal analysis, C.T., A.M. and G.M.; investigation, M.G.S. and F.C.; data curation, C.T. and A.M.; writing—original draft preparation, M.G.S.; writing—review and editing, M.G.S., G.M. and R.P.; visualization, M.G.S. and R.A.; supervision, M.G.S. and R.P.; project administration, M.G.S. All authors have read and agreed to the published version of the manuscript.

**Funding:** This research received no external funding.

**Institutional Review Board Statement:** Not applicable.

**Informed Consent Statement:** Not applicable.

**Data Availability Statement:** Data is available on the request from the corresponding author.

**Conflicts of Interest:** The authors declare no conflict of interest.

## References


1. Acquaviva, R.; Sorrenti, V.; Santangelo, R.; Cardile, V.; Tomasello, B.; Malfa, G.; Vanella, L.; Amodeo, A.; Genovese, C.; Mastrojeni, S.; et al. Effects of an extract of *Celtis aetnensis* (Tornab.) Strobl twigs on human colon cancer cell cultures. *Oncol. Rep.* **2016**, *36*, 2298–2304. [CrossRef] [PubMed]
2. Bonesi, M.; Loizzo, M.R.; Acquaviva, R.; Malfa, G.; Aiello, F.; Tundis, R. Anti-inflammatory and antioxidant agents from *Salvia genus* (Lamiaceae): An assessment of the current state of knowledge. *Antiinflamm. Antiallergy Agents Med. Chem.* **2017**, *16*, 70–86. [CrossRef] [PubMed]
3. Malfa, G.A.; Tomasello, B.; Acquaviva, R.; Genovese, C.; La Mantia, A.; Cammarata, F.P.; Ragusa, M.; Renis, M.; Di Giacomo, C. *Betula etnensis* Raf. (Betulaceae) extract induced HO-1 expression and ferroptosis cell death in human colon cancer cells. *Int. J. Mol. Sci.* **2019**, *20*, 2723. [CrossRef]
4. Tomasello, B.; Malfa, G.A.; La Mantia, A.; Miceli, N.; Sferrazzo, G.; Taviano, M.F.; Di Giacomo, C.; Renis, M.; Acquaviva, R. Anti-adipogenic and anti-oxidant effects of a standardised extract of Moro blood oranges (*Citrus sinensis* (L.) Osbeck) during adipocyte differentiation of 3T3-L1 preadipocytes. *Nat. Prod. Res.* **2019**, *9*. [CrossRef]
5. Naoi, M.; Inaba-Hasegawa, K.; Shamoto-Nagai, M.; Maruyama, W. Neurotrophic function of phytochemicals for neuroprotection in aging and neurodegenerative disorders: Modulation of intracellular signaling and gene expression. *J. Neural Transm.* **2017**, *24*, 1515–1527. [CrossRef] [PubMed]
6. Rehman, M.U.; Wali, A.F.; Ahmad, A.; Shakeel, S.; Rasool, S.; Ali, R.; Rashid, S.M.; Madkhali, H.; Ganaie, M.A.; Khan, R. Neuroprotective Strategies for Neurological Disorders by Natural Products: An update. *Curr. Neuropharmacol.* **2019**, *17*, 247–267. [CrossRef]
7. Teleanu, R.I.; Chircov, C.; Grumezescu, A.M.; Volceanov, A.; Teleanu, D.M. Antioxidant therapies for neuroprotection—A review. *J. Clin. Med.* **2019**, *8*, 1659. [CrossRef]
8. Su, P.; Shi, Y.; Wang, J.; Shen, X.; Zhang, J. Anticancer agents derived from naturalcinnamic acids. *Anticancer Agents Med. Chem.* **2015**, *15*, 980–987. [CrossRef] [PubMed]
9. Chen, C. Sinapic acid and its derivatives as medicine in oxidative stress-induced diseases and aging. *Oxidative Med. Cell Longev.* **2016**, 3571614. [CrossRef]
10. Zhang, Q.; Hu, J.X.; Kui, X.; Liu, C.; Zhou, H.; Jiang, X.; Zeng, L. Sinapic Acid Derivatives as Potential Anti-Inflammatory Agents: Synthesis and Biological Evaluation. *Iran. J. Pharm. Res.* **2017**, *16*, 1405–1414.
11. Kulkarni, M.G.; Rengasamy, K.R.R.; Pendota, S.C.; Gruz, J.; Plačková, L.; Novák, O.; Doležal, K.; Van Staden, J. Bioactive molecules derived from smoke and seaweed *Ecklonia maxima* showing phytohormone-like activity in *Spinacia oleracea* L. *New Biotechnol.* **2019**, *48*, 83–89. [CrossRef]
12. Milkowski, C.; Strack, D. Sinapate esters in brassicaceous plants: Biochemistry, molecular biology, evolution and metabolic engineering. *Planta* **2010**, *232*, 19–35. [CrossRef]
13. Hameed, H.; Aydinj, S.; Basaran, N. Sinapic Acid: Is It Safe for Humans? *Pharm. Sci.* **2016**, *41*, 39–49.
14. Bagli, E.; Goussia, A.; Moschos, M.M.; Agnantis, N.N.; Kitsos, G. Natural compounds and neuroprotection: Mechanisms of action and novel delivery systems. *In Vivo* **2016**, *30*, 535–547.
15. Castelli, F.; Messina, C.; Sarpietro, M.G.; Pignatello, R.; Puglisi, G. Flurbiprofen release from Eudragit RS and RL aqueous nanosuspensions: A kinetic study by DSC and dialysis experiments. *AAPS PharmSciTech* **2002**, *3*, 26–33. [CrossRef]
16. Berrío Escobar, J.F.; Pastrana Restrepo, M.H.; Márquez Fernández, D.M.; Martínez Martínez, A.; Giordani, C.; Castelli, F.; Sarpietro, M.G. Synthesis and interaction of sterol-uridine conjugate with DMPC liposomes studied by differential scanning calorimetry. *Colloids Surf. B Biointerfaces* **2018**, *166*, 203–209. [CrossRef]
17. Sarpietro, M.G.; Accolla, M.L.; Puglisi, G.; Castelli, F.; Montenegro, L. Idebenone loaded solid lipid nanoparticles: Calorimetric studies on surfactant and drug loading effects. *Int. J. Pharm.* **2014**, *471*, 69–74. [CrossRef]
18. Montenegro, L.; Ottimo, S.; Puglisi, G.; Castelli, F.; Sarpietro, M.G. Idebenone loaded solid lipid nanoparticles interact with biomembrane models: Calorimetric evidence. *Mol. Pharm.* **2012**, *9*, 2534–2541. [CrossRef] [PubMed]
19. Montenegro, L.; Castelli, F.; Sarpietro, M.G. Differential Scanning Calorimetry analyses of idebenone-loaded solid lipid nanoparticles interactions with a model of bio-membrane: A comparison with in vitro skin permeation data. *Pharmaceuticals* **2018**, *11*, 138. [CrossRef] [PubMed]
20. Dudhipala, N.; Veerabrahma, K. Improved anti-hyperlipidemic activity of Rosuvastatin Calcium via lipid nanoparticles: Pharmacokinetic and pharmacodynamic evaluation. *Eur. J. Pharm. Biopharm.* **2017**, *110*, 47–57. [CrossRef]
21. Cevc, G. Polymorphism of the bilayer membranes in the ordered phase and the molecular origin of the lipid pretransition and rippled lamellae. *Biochim. Biophys. Acta* **1991**, *1062*, 59–69. [CrossRef]
22. Lewis, R.N.A.H.; McElhaney, R.N. The mesomorphic phase behavior of lipids bilayers. In *The Structure of Biological Membranes*; Yeagle, P.L., Ed.; CRC Press: Boca Raton, FL, USA, 1992; Chapter 2; pp. 73–155.
23. Jørgensen, K.; Ipsen, J.H.; Mouritsen, O.G.; Bennett, D.; Zuckermann, M.J. A general model for the interaction of foreign molecules with lipid membranes: Drugs and anaesthetics. *Biochim. Biophys. Acta* **1991**, *1062*, 227–238. [CrossRef]
24. Jørgensen, K.; Ipsen, J.H.; Mouritsen, O.G.; Bennett, D.; Zuckermann, M.J. The effects of density fluctuations on the partitioning of foreign molecules into lipid bilayers: Application to anaesthetics and insecticides. *Biochim. Biophys. Acta* **1991**, *1067*, 241–253. [CrossRef]